

UHASSELT



Maastricht University

KNOWLEDGE IN ACTION

Faculty of Medicine and Life Sciences
School for Life Sciences

Master of Biomedical Sciences

Master's thesis

The effect of pericyte changes on the glymphatic system in the EAE mouse model

Brecht Moonen

Thesis presented in fulfillment of the requirements for the degree of Master of Biomedical Sciences, specialization
Molecular Mechanisms in Health and Disease

SUPERVISOR :

Prof. dr. Bieke BROUX

SUPERVISOR :

Dr. Iben LUNDGAARD

MENTOR :

Na LIU

Transnational University Limburg is a unique collaboration of two universities in two countries: the University of Hasselt and Maastricht University.



UHASSELT

KNOWLEDGE IN ACTION

www.uhasselt.be

Universiteit Hasselt
Campus Hasselt:
Martelarenlaan 42 | 3500 Hasselt
Campus Diepenbeek:
Agoralaan Gebouw D | 3590 Diepenbeek

2022
2023



UHASSELT

KNOWLEDGE IN ACTION



Maastricht University

Faculty of Medicine and Life Sciences

School for Life Sciences

Master of Biomedical Sciences

Master's thesis

The effect of pericyte changes on the glymphatic system in the EAE mouse model

Brecht Moonen

Thesis presented in fulfillment of the requirements for the degree of Master of Biomedical Sciences, specialization
Molecular Mechanisms in Health and Disease

SUPERVISOR :

Prof. dr. Bieke BROUX

SUPERVISOR :

Dr. Iben LUNDGAARD

MENTOR :

Na LIU

The effect of pericyte changes on the glymphatic system in the EAE mouse model

Brecht Moonen, Na Liu^{1,2}, Bieke Broux³, Niels Hellings³, Iben Lundgaard^{1,2}

¹Department of Experimental Medical Science, Lund University, Lund, Sweden

²Wallenberg Centre for Molecular Medicine, Lund University, Lund, Sweden

³Hasselt University, Biomedical Research Institute and transnationale Universiteit Limburg, School of Life Sciences, Agoralaan, Building C, 3590 Diepenbeek, Belgium

*Running title: *Pericyte changes on glymphatics in EAE mice*

To whom correspondence should be addressed: Iben Lundgaard, Tel: +46 (0) 46 222 0621; Email: Iben.Lundgaard@med.lu.se

Keywords: *Multiple sclerosis, experimental autoimmune encephalomyelitis (EAE), glymphatic system, pericytes, light-sheet microscopy*

ABSTRACT

Multiple sclerosis (MS) is the most common non-traumatic neurodegenerative disease of the central nervous system (CNS) in young adults. Thus far, there is no curative treatment for MS, indicating a clear need for research into the pathological mechanisms of MS to provide a clear focus for developing novel therapies. The glymphatic system is a recently discovered waste clearance pathway in the CNS. It comprises a network of perivascular channels surrounded by astrocytic endfeet that facilitate cerebrospinal fluid (CSF) movement throughout the brain. Pericytes are mural cells that are in close association with these channels. We hypothesize that their dysfunction lies at the heart of glymphatic system and blood-brain barrier (BBB) dysfunction. By means of immunohistochemical analysis, we found that blood vessel-associated pericyte loss in the experimental autoimmune encephalomyelitis (EAE) model is accompanied by BBB disruption. This was indicated by decreased claudin-5 expression and Evans Blue dye leakage across the BBB. Furthermore, we find that pericytes might play a role in regulating the expression of AQP4, a critical regulator of the glymphatic system. Lastly, using the novel method of whole brain clearing and light sheet microscopy, we find that the glymphatic system is implicated in the chronic stages of EAE. This study is a significant step forward in our

understanding of the role of pericytes in maintaining BBB integrity and glymphatic function. By elucidating these mechanisms, we deepen our comprehension of MS pathogenesis and pave the way for innovative therapeutic interventions targeting pericytes.

INTRODUCTION

Multiple sclerosis (MS) is the most prevalent chronic autoimmune neurodegenerative disease of the central nervous system (CNS), affecting 2.8 million people worldwide. MS is most commonly diagnosed in young adults and mainly affects women (1, 2). In this disease, tolerance for the myelin sheath surrounding the axons is lost, resulting in widespread demyelination, chronic inflammation, and neuronal loss (1, 2). This often leads to symptoms such as fatigue, forgetfulness, and mobility issues. Various subtypes of MS exist based on the progression of the disease. The most common disease course follows a remitting-relapsing pattern (RRMS). However, due to the hampered ability of the endogenous repair systems to properly remyelinate the damaged myelin sheath, neurological and cognitive deterioration will occur over time (2). Therefore, many patients ultimately develop into a progressive state (PSMS) (2). Lastly, primary progressive MS (PPMS) is a rare subtype that occurs only in 10-15% of MS patients (1). A progressive cognitive decline at the initial onset of the disease characterizes this subset. Thus far, there is no cure for MS; current therapies focus solely on

symptomatic alleviation and stalling cognitive and neurological decline (1, 3, 4). There are currently disease-modifying therapies available; however, they are typically employed as a second line of treatment due to the potential for severe side effects. For example, alemtuzumab, an antibody that targets CD52, has been associated with severe adverse reactions in 1-3% of the individuals participating in studies, and in some cases, it has even resulted in fatalities (5). Therefore, there is a clear need for research into the pathological mechanisms of MS to provide a clear focus for developing novel therapies.

The most crucial pathological hallmark of MS is the disruption of the blood-brain barrier (BBB)(6, 7). The BBB represents a cellular barrier between the blood and the brain parenchyma. It comprises endothelial cells, pericytes, and their basal lamina, surrounded and supported by astrocytes and perivascular macrophages (6, 7). This heavily restrictive barrier allows tight regulation of CNS homeostasis and protects against the entry of xenobiotics, toxic metabolites, and immune cells into the CNS (7, 8). The breakdown of this barrier in the MS pathology leads to altered signaling homeostasis and increased infiltration of neutrophils, macrophages, and toxic metabolites, enhancing neuroinflammation and demyelination (6, 8). Unfortunately, the exact mechanism and time point at which BBB breakdown happens has remained unknown. Literature suggests that pericytes play a crucial role in maintaining BBB Integrity. Pericytes are mural cells embedded within the walls of capillaries throughout the body, including the brain (9). They are thought to maintain BBB integrity by communicating with endothelial cells of the cerebral capillaries through forming gap- and adherence-junctions (10, 11). Additionally, they have been identified to play an essential role in regulating cerebral blood flow through their contractile properties (9, 10). From this, we speculate that neuroinflammation, as seen in MS, induces damage to pericytes, reducing their function as well as their total numbers. We suspect that this in turn is a driving factor in the breakdown of the BBB. Subsequently, this may result in the leakage of serum proteins into the CNS parenchyma, causing edema and compression of the cerebral microvasculature (12). Experimental autoimmune encephalomyelitis (EAE) is a commonly used animal model that mimics features

of MS, including the breakdown of the BBB and infiltration of immune cells into the CNS. Interestingly, shrinking of the cerebral and spinal vasculature and reduced blood perfusion is often described in the EAE mouse model and MS patients, especially during BBB breakdown (12, 13).

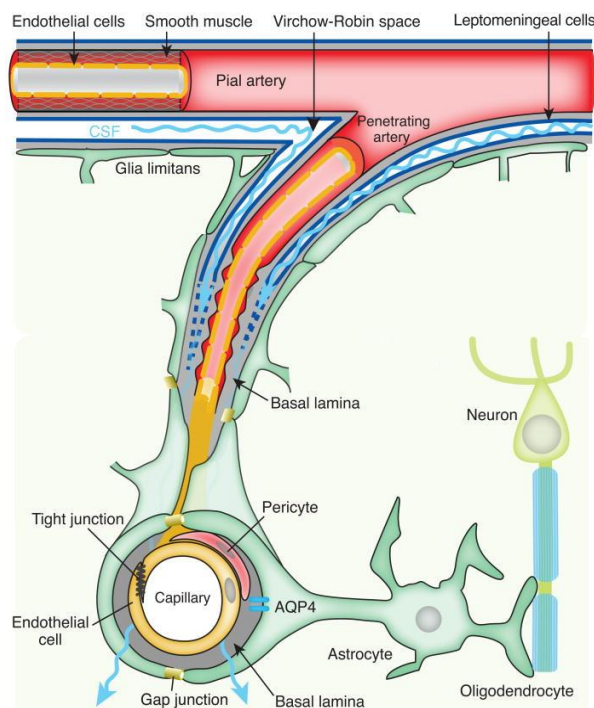


Figure 1: the neurovascular unit. Pial arterioles in the subarachnoid space become penetrating arteries upon diving into the brain parenchyma. As the penetrating arteries branch into arterioles and capillaries, the CSF-containing Virchow-Robin spaces narrow and finally disappear. However, the perivascular space extends to arterioles and capillaries to venules, which comprises the basal lamina's extracellular matrix that provides a continuity of the fluid space between arterioles and venules. Astrocytic vascular endfeet surround the entire vasculature and forms the boundary of the perivascular spaces — figure from Jessen et al. (14).

As the major arteries of the brain descend into the brain parenchyma, they transition into penetrating arterioles and develop a perivascular space. This space resembles a donut-shaped tunnel surrounding the penetrating arteries and is also known as the Virchow-Robin space. It transports the cerebral spinal fluid (CSF) and is bordered by an outer wall comprising perivascular astrocytic end feet, as shown in Figure 1 (14). As the penetrating arteries transition into cerebral capillaries, the perivascular space becomes continuous with the basal lamina.

Recent studies have demonstrated that CSF and the brain's interstitial fluid continuously interchange (15). Movement of the CSF from the perivascular space into the parenchyma drives the interstitial fluid containing biological waste toward the perivenous spaces surrounding the large deep veins (14). Subsequently, the waste-containing interstitial fluid may then be discarded. This system is called the glymphatic system. It is responsible for the clearance of soluble waste proteins and interstitial metabolites and is crucial for maintaining proper brain function (16).

Recently it has been discovered that the glymphatic system is impaired in MS patients. It has been indicated that these patients show lower overall diffusion of CSF along the perivascular space, especially in the progressive stages of the disease (13). Furthermore, decreased CSF flow along the perivascular space was associated with increased clinical disability and longer relapse duration (13). Reduced clearance of biological waste products by the glymphatic system might induce the inflammation and neurodegeneration seen in these MS patients (12). Furthermore, clearance of myelin debris is necessary for effective remyelination and repair of neuronal circuits to occur (17, 18). This leads us to believe that impairment of the glymphatic system is a pathological mechanism underpinning MS. The main driving factor for CSF flow along the perivascular space is the perfusion of the cerebral capillaries (19). The cardiac cycle generates pulsatile movements along the capillary wall, which propels the CSF in the perivascular space forward (19). However, as described before, the blood flow perfusion is impaired in MS due to BBB breakdown, for which we suspect the loss of pericyte function to be responsible. In addition to this, pericytes have contractile properties; they generate pulsatile waves along the length of the perivascular space, which aids CSF flow (19, 20). Furthermore, recent discoveries have described that pericytes form precapillary sphincters that control cerebral blood flow (21). We suspect this system to be compromised during the onset of MS as well.

Knowledge of how pericytes contribute to vascular and glymphatic dysfunction during the development of neurodegenerative diseases such as MS has remained limited. **The aim of this study** is to provide an understanding of the mechanisms that underlie pericyte and glymphatic dysfunction in the

EAE mouse model which may provide new insights into the pathogenesis of MS. **We hypothesize** that early EAE induction will negatively affect pericyte function, reducing BBB integrity, resulting in glymphatic impairment. In this paper, we use immunohistochemical analysis to determine the effect of EAE induction on pericyte density and coverage of the cerebral in the dorsal cortex and spinal cord. Additionally, we sought to determine whether these pericyte changes alter BBB permeability and expression of proteins necessary for the formation of tight junctions and effective CSF transport across the perivascular space. Lastly, we make use of the novel technique of light-sheet microscopy (22). This technique allows us to spatially analyze the glymphatic system by generating a three-dimensional image of optically cleared brains from EAE-induced mice.

EXPERIMENTAL PROCEDURES

Mice

Wild-type (WT) C57BL/6 mice were purchased from Charles River Laboratories. Animals were housed in the animal facility of the BMC biomedical center of Lund University. All experiments were performed according to institutional guidelines and were approved by the ethical committee of Lund University.

EAE induction

To induce EAE, C57BL/6 mice were injected subcutaneously at the flank of the back with 200 μ L of emulsion. The emulsions consisted of 50 μ g mouse MOG₃₅₋₅₅ peptide and 200 μ g mycobacterium tuberculosis H37RA, emulsified in Complete Freund's Adjuvant (CFA), provided by Thomas Bäckström. The emulsion was injected under anesthesia, using isoflurane (ISO) (induction at 3%, maintained at 2% for the duration of the experiment) in atmospheric air (70.9% N₂, 20% O₂, 0.1% CO). Bordella Pertussis toxin (Sigma-Aldrich) in saline was injected intraperitoneally 2h and 24h post-induction. The mice were checked daily for symptoms using a scale ranging from 0-5, according to Ramos-Vega et al (12).

Evans blue dye and cisternal tracer injections

EAE-induced mice were sacrificed during the pre-symptomatic phase (8 days post-induction; DPI), the acute phase (16 DPI), and the chronic phase (25-26 DPI). Prior to sacrifice, all mice were injected

intraperitoneally (IP) with 150mg/kg (2% w/v solution) Evans Blue (Sigma-Aldrich). The Evans Blue dye was allowed to circulate for 2h. One mouse per group received a cisterna magna (CM) injection. These were performed under general anesthesia induced through IP injection of ketamine/xylazine (KX), 100 mg/kg/20 mg/kg. Next, an incision at the back of the skull was made to reveal the cisterna magna. The core temperature was kept at 37°C using a heating pad connected to a rectal feedback probe. The CM injection was carried out with a 30 G dental needle (Carpule, Sopira) connected to a 100 µL Hamilton syringe via PE10 tubing. 10 µL of 1% AlexaFluor488-conjugated bovine serum albumin (BSA-488, Invitrogen) tracer was injected into the CM at 1 µL/min using a KDS Legato 100 single infusion syringe pump. After injection, the tracer was allowed to circulate for 30 min. *In vivo* imaging was performed during the 30-min circulation time using a Nikon SMZ25 microscope. Subsequently, all mice were intracardially perfused with phosphate-buffered saline (PBS) followed by 4% paraformaldehyde (PFA) for fixation. The intracardial injection was performed either manually using a 50ml syringe or automatically using a peristaltic pump (Watson-Marlow 120 series) set at 30 RPM. The brain and spinal cord were extracted and post-fixed in 4% PFA for 24h. The brains and spinal cord were finally imaged again with the Nikon SMZ25 microscope.

Tissue processing

The brain and spinal cord were cut into 100µm slices using the Leica VT1000 Vibratome. To this end, the spinal cords were embedded into a 2% agarose gel (supplier) prepared with Tris-Borate-EDTA (TBE) buffer. The agarose gel was allowed to cool down below 36°C prior to embedding. Slicing was performed at a speed of 1mm/s with an amplitude of 1mm for both brain and spinal cord tissue. The brain and spinal cord slices were stored at 4°C in 1xPBS containing 0.1% sodium-azide.

Immunohistochemistry

For particular antigens (See Suppl. Table 1), antigen retrieval was performed. To this end, the brain and spinal cord slices were incubated at 60°C overnight in 1xPBS containing sodium citrate set to a pH of 6. The brain and spinal cord slices were then blocked for 3h at room temperature using blocking

buffer containing 1xPBS, 1% BSA (Sigma-Aldrich), 5% normal donkey serum (Jackson Immunoresearch), 0,5% Tween-20 (Sigma-Aldrich) and 0.5% Triton X-100 (Sigma-Aldrich). The slices were subsequently stained overnight at 4°C with the relevant primary antibodies (See Suppl. Table 1) diluted in 1:1 PBS and blocking buffer. Next, the slices were stained using the appropriate secondary antibodies (see Suppl. table 1) and diluted in PBS. Lastly, brain slices were mounted on glass slides with Fluorescence Mounting Medium (Invitrogen) and imaged using the Nikon A1RHD Confocal Microscope. Finally, the results were analyzed using ImageJ software.

Optical tissue clearing and light-sheet imaging

To optically clear the tissue, the iDISCO+ protocol was carried out as described by Renier et al. (23). Brain tissue was dehydrated using a methanol/H₂O series (20%, 40%, 60%, 80%, 100%, 100%, 1 h each). The tissue was left in 100% methanol overnight. Next, the tissue was delipidated with methanol/dichloromethane (DCM) 33%/66% for 3 h and 100% DCM 2 x 15 min. Finally, the brain tissue was optically cleared ethyl-cinnamate (ECi) for at least 24h before imaging. The brain samples were imaged using an Ultramicroscope II light-sheet microscope (LaVision Biotech) with a 1.3× LaVision LVMI-Fluor lens (0.105 NA) equipped with an sCMOS camera (Andor Neo, model 5.5-CL3). Brains were imaged immersed in ECi in the transverse orientation at a z-step size of 5 µm with InspectorPro64 (LaVision Biotech). Several stacks (mosaic acquisition) were taken with 10% overlap to image the entire brain. 3D renditions and movies were created with Arivis Vision 4 D 3.1 (Arivis AG). Alternatively, tissues were cleared with the CUBIC (clear, unobstructed brain/body imaging cocktails and computational analysis) method. First, the brain samples were delipidated over 5 days with CUBIC-L (10%wt N-butyl diethanolamine (Sigma-Aldrich), 10% triton X-100 (Sigma-Aldrich)). Incubation was done shielded from light at 36°C while gently shaking. The CUBIC-L solution was refreshed every other day. Next, the brain samples were incubated in 1:1 CUBIC-R+ (45%wt antipyrine (Sigma-Aldrich), 30%wt nicotinamide (Sigma-Aldrich) in water, buffered with 0,05% (v/w) N-butyl diethanolamine (pH10)) and MilliQ for one day at room temperature while gently shaking. Brains were

imaged immersed in 1:1 mineral oil (Sigma-Aldrich) and silicone oil (supplier) in the transverse orientation at a z-step size of 5 μm with InspectorPro64 (LaVision Biotec). Several stacks (mosaic acquisition) were taken with 10% overlap to image the entire brain. 3D renditions and movies were created with Arivis Vision 4D 3.1 (Arivis AG).

Statistical analysis

Statistical analysis of the data was done using GraphPad Prism 9. The normality of the data was evaluated using the Shapiro-Wilk test. If the data exhibited a normal distribution, an ANOVA with Tukey's post hoc analysis was conducted. Conversely, if the data did not follow a normal distribution either the Mann-Whitney or Kruskal-Wallis test was performed instead. We considered P-values less than 0.05 to indicate a significant difference.

RESULTS

EAE induction leads to decreased pericyte density and vessel coverage

Recent studies have highlighted the occurrence of alterations in pericytes under stress conditions, leading to structural and functional modifications (9, 24, 25). However, the specific nature of pericyte alterations in the EAE model has remained unclear. To address this knowledge gap, we conducted an experiment using C57BL/6 mice, inducing EAE by administering CFA/MOG₃₅₋₅₅ injections. Throughout the experiment, we monitored the mice daily and recorded their disease scores to assess the progression of EAE. The mice were sacrificed at various stages of the disease. This experimental design allowed us to investigate the changes occurring in pericytes during different phases of EAE and gain insights into their role in disease pathogenesis. By elucidating the alterations in pericytes within the EAE model, this experiment aimed to enhance our understanding of the underlying mechanisms driving neuroinflammation and disease progression.

In this first experiment, pericytes located in the dorsal cortex were subjected to immunostaining for CD13 and PDGFRb, as depicted in Figure 1A. Simultaneously, blood vessels were stained using *Lycopersicon esculentum* (Tomato) Lectin, DyLight 488 to visualize their presence. Notably, as the EAE model progressed, a significant

decrease in the CD13 expression was observed (Figure 1B). Conversely, there were no notable alterations in the lectin + area (Figure 1C), suggesting that there are no evident vascular abnormalities in the cortex. However, a reduction in both the pericyte count (Figure 1D) and pericyte vessel coverage (Figure 1E) was observed, suggesting a potential disruption in the pericyte population and their association with blood vessels in the cortical region. During the quantification process, we observed a minor non-specific staining by lectin. Nevertheless, this does not impact the quantification results since the overlapping signal between the background lectin staining and the background signal from the CD13 staining does not surpass the threshold required for colocalization. Pericytes located in the thoracic spinal cord were similarly subjected to immunohistochemical staining using CD13, as illustrated in Figure 1F. In addition, blood vessels were visualized using Dylight-488 labeled Tomato Lectin. Unlike in the cortex, there was no significant decrease observed in the CD13 expression (Figure 1F). However, a significant decrease in the pericyte vessel coverage was observed (Figure 1I). Interestingly, during the acute phase of the EAE model, we noted a significant increase in the lectin+ area, indicating the presence of vascular abnormalities (Figure 1H). To confirm the specificity of lectin staining in the spinal cord during the acute phase, we performed colocalization analysis with CD31, a marker for vascular endothelial cells. Supplementary Figure 1 shows the colocalization of lectin and CD31 in the thoracic spinal cord during the acute phase, demonstrating that lectin staining is indeed specific in this context. Similar vascular changes were observed during the chronic phase, although this did not result in a significant increase in the lectin+ area (Figure 1F, G).

Claudin-5 expression is lost in the progressive stages of EAE

The integrity of the BBB is crucial for maintaining the homeostasis of the CNS and protecting it from harmful substances (8). One key aspect of BBB maintenance is the formation of tight junctions between endothelial cells. Alterations in pericyte function and communication with endothelial cells can lead to compromised tight junction integrity, facilitating the infiltration of immune cells into the CNS (26). In the context of EAE, the involvement

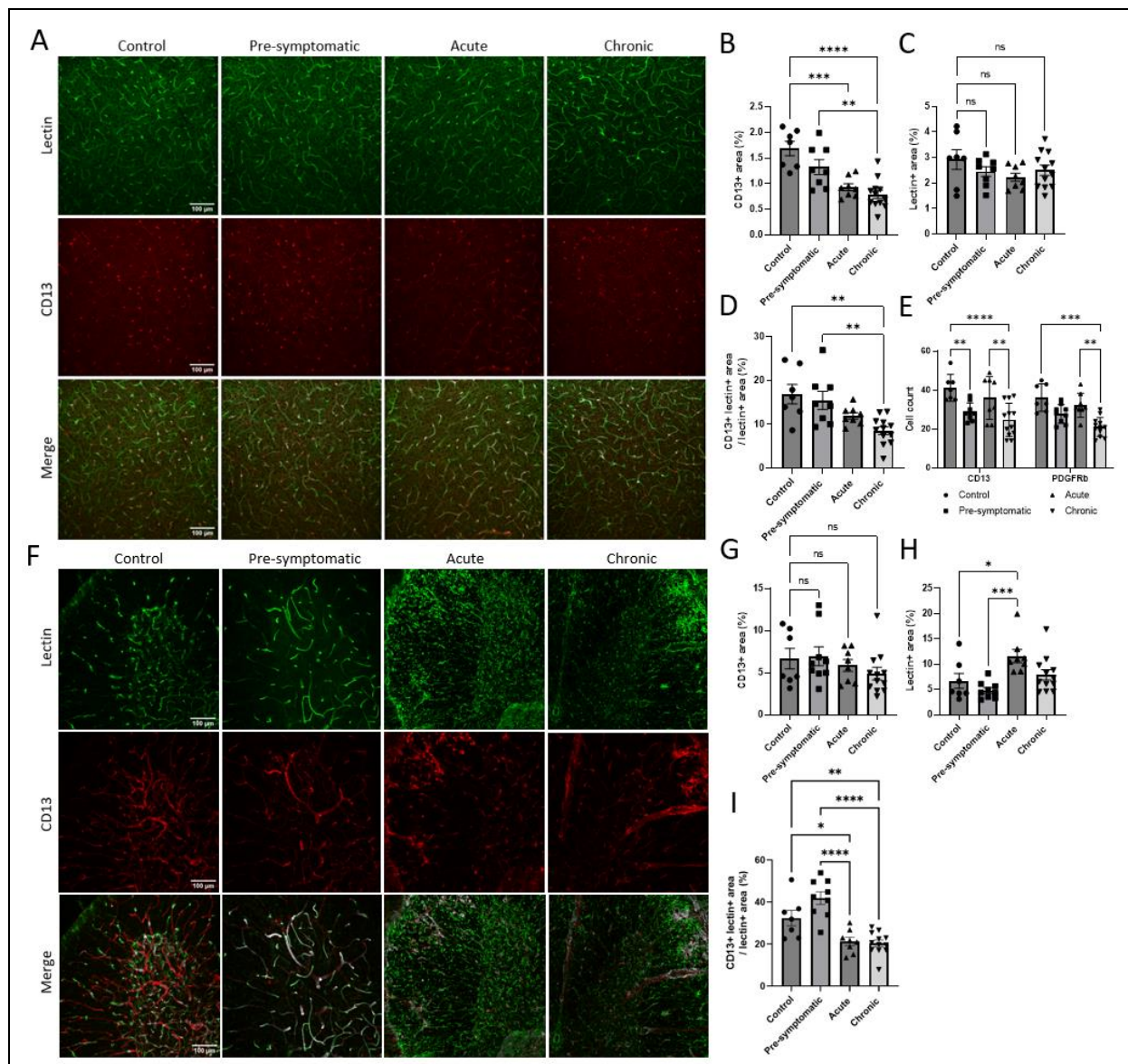
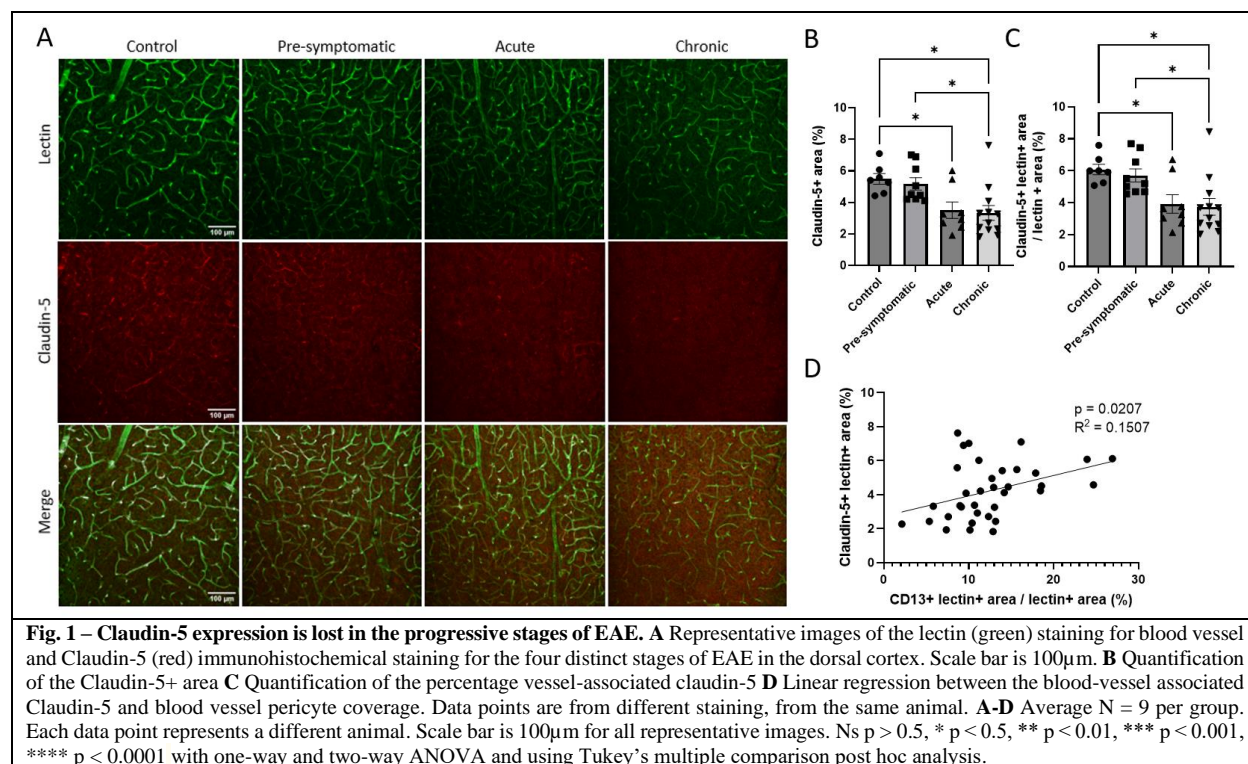


Fig. 1 – EAE induction leads to decreased pericyte density and vessel coverage. **A** Representative images of lectin (green) staining and CD13 (red) immunohistochemical staining for blood vessels and pericytes respectively for the four distinct stages of EAE in the dorsal cortex. Scale bar is 100µm. **B** Quantification of CD13+ area in the dorsal cortex **C** Quantification of the lectin + area in the dorsal cortex **D** Quantification of the blood vessel pericyte coverage in the dorsal cortex **E** Number of CD13+ and PDGFRb+ cells in the dorsal cortex **F** Representative images of the lectin (green) staining and CD13 (red) immunohistochemical staining for blood vessels and pericytes respectively for the four distinct stages of EAE in the thoracic spinal cord. Scale bar is 100µm **G** Quantification of CD13+ area in the thoracic spinal cord **H** Quantification of the lectin+ area in the thoracic spinal cord **I** Quantification of the blood vessel pericyte coverage in the thoracic spinal cord. **A-I** Average N = 9 per group. Each data point represents a different animal. Ns p > 0.5, * p < 0.5, ** p < 0.01, *** p < 0.001, **** p < 0.0001 with one-way and two-way ANOVA and using Tukey’s multiple comparison post hoc analysis.

of pericytes in BBB dysfunction and breakdown has attracted significant research interest. Understanding the mechanisms underlying the interplay between pericytes and tight junctions in EAE can provide valuable insights into the pathogenesis of MS. Therefore, this experiment aims to investigate the role of pericytes in EAE-related BBB disruption, focusing on the expression of claudin-5, a critical component of tight junctions,

and its association with pericytes. By employing immunohistochemical techniques and analyzing tissue samples from EAE animal models sacrificed at different stages of the disease, we aim to elucidate the impact of pericyte-mediated changes on BBB integrity and their contribution to disease progression. In Figure 2A, immunohistochemical staining was performed to assess claudin-5 expression in the



cortex. Additionally, Dylight-488 labeled Tomato Lectin was used to visualize blood vessels. A significant decrease in total claudin-5 expression was observed in mice during the acute and chronic stages of the disease, indicating disrupted BBB integrity (Figure 2B). To account for potential microglia-related parenchymal claudin-5 expression, claudin-5 expression colocalized with lectin was measured. Similarly, a decrease in vessel-associated claudin-5 expression was observed in the mice that had entered the acute and chronic stage of EAE, further indicating compromised BBB integrity (Figure 2C). Correlating these findings with pericyte vessel coverage revealed a positive association between claudin-5 expression and pericyte coverage (Figure 2D). These results suggest the vital role of pericytes in maintaining claudin-5 expression and preserving BBB integrity.

EAE inductions leads to BBB leakage in the pre-symptomatic phase, evidenced by EB extravasation

Our findings suggest that pericytes might play a pivotal role in maintaining the selective permeability of the BBB by maintaining claudin-5 expression. This loss of BBB integrity may result in BBB leakage. Understanding the involvement of

pericytes in EAE-related BBB leakage is of significant interest as this can provide valuable insights into the underlying mechanisms of neuroinflammation and MS pathogenesis. Therefore, we employed the Evans Blue (EB) dye extravasation method elucidate the potential relationship between pericyte alterations and the extent of BBB leakage in EAE.

Quantification of EB dye in the dorsal cortex using *ex vivo* epifluorescence imaging of the whole brain provided valuable insights into BBB permeability changes during the different phases of EAE (Figure 3A). To this end, all brains were imaged immediately after perfusion in mice injected with Evans Blue dye (Figure 3B). We observed an elevation in total EB content both in the dorsal and ventral cortex of EAE mice during the pre-symptomatic phase (Figure 3C). Additionally, we performed confocal microscopy to quantify EB dye in the dorsal cortex (Figure 3D). Consistent with the results from *ex vivo* fluorescent imaging, we observed an increased amount of total EB in the dorsal cortex during the pre-symptomatic phase of EAE, indicating enhanced BBB permeability (Figure 3E). Although there were no significant changes in the lectin+ area in the dorsal cortex during EAE disease progression. We conducted an additional analysis to correct for the effect of

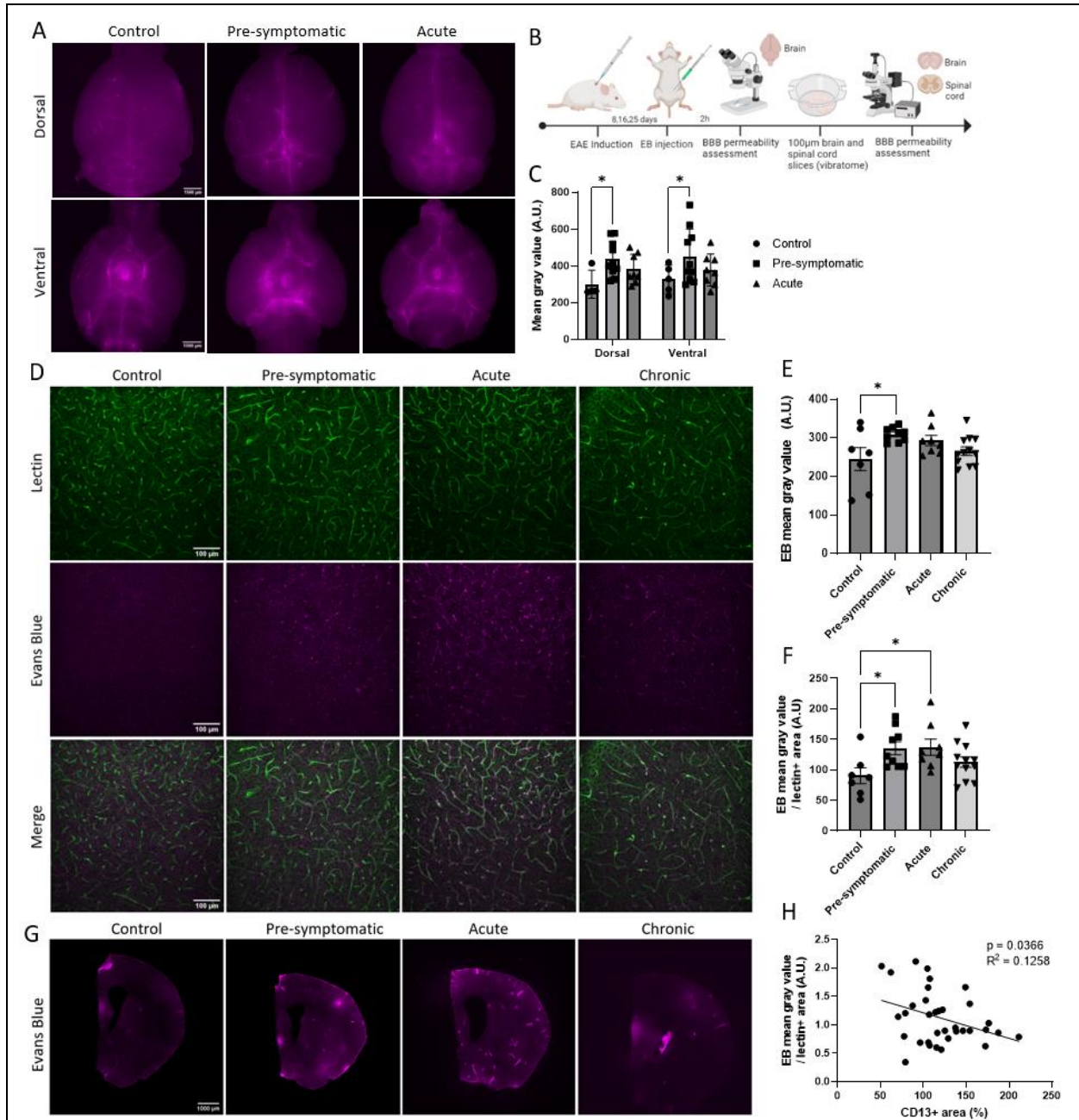
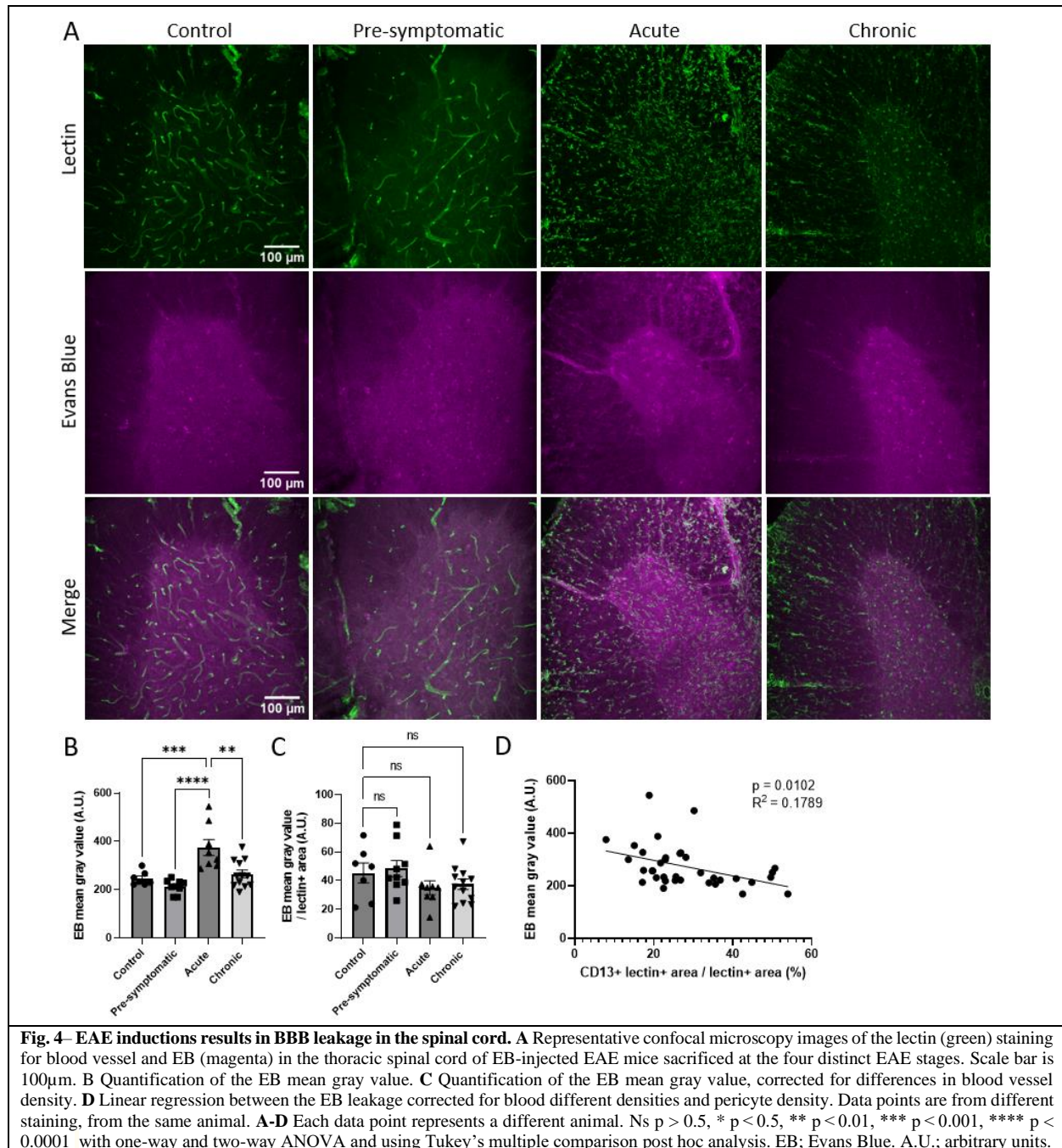


Fig. 3 – EAE induction leads to BBB leakage in the dorsal cortex, evidenced by EB extravasation. **A** Representative images of *ex vivo* epifluorescence imaging of the dorsal and ventral regions of whole brains from EB injected EAE mice sacrificed at the pre-symptomatic and acute stages. Scale bar 1500µm. N= 4-5 for control groups, N = 10 for Pre-symptomatic groups and N=8 for acute groups. Few controls were excluded due to imaging errors resulting in extremely high gray values. **B** Illustration of experimental setup **C** Quantification of the mean gray value of the dorsal and ventral region after *ex vivo* epifluorescence imaging. **D** Representative confocal microscopy images of the lectin (green) staining for blood vessel and EB (magenta) in the dorsal cortex of EB-injected EAE mice sacrificed at the four distinct EAE stages. Scale bar is 100µm. **E** Quantification of the EB mean gray value. **F** Quantification of the EB mean gray value, corrected for differences in blood vessel density. **G** Representative images of widefield fluorescence imaging of EB (magenta) in the dorsal cortex of EB-injected EAE mice sacrificed at the four distinct EAE stages. Scale bar is 1000µm. **H** Linear regression between the EB leakage corrected for blood different densities and pericyte density. Data points are from different staining, from the same animal. **D-H** Average N = 9 per group. Each data point represents a different animal. Ns $p > 0.5$, * $p < 0.5$, ** $p < 0.01$, *** $p < 0.001$, **** $p < 0.0001$ with one-way and two-way ANOVA and using Tukey’s multiple comparison post hoc analysis. EB; Evans Blue. A.U.; arbitrary units.

possible vascular changes, considering the tendency of EB dye to bind to the blood vessel wall.

This analysis demonstrated an elevated level of EB extravasation in both the pre-symptomatic and



acute phases of EAE (Figure 3F). Additionally, to exclude the possibility that our fast manual perfusion method induces artificial BBB leakage, we compared the EB dye signal in healthy control mice that were perfused either manually to mice that were perfused slowly with a peristaltic pump and heparinized PBS. Here we confirmed that our manual perfusion method does not induce artificial leakage and more effectively removes EB dye remaining in the blood vessel (Supplemental figure

2). By employing widefield fluorescence microscopy, we observed focal sites of BBB leakage in brain slices obtained from mice in the pre-symptomatic and acute phases of EAE (Figure 3G). To elucidate the potential role of pericyte dysfunction in BBB alterations, we correlated these findings with immunohistochemical staining for CD13, a marker for pericytes in the cortex. Our analysis revealed a positive association between decreased pericyte coverage and increased EB

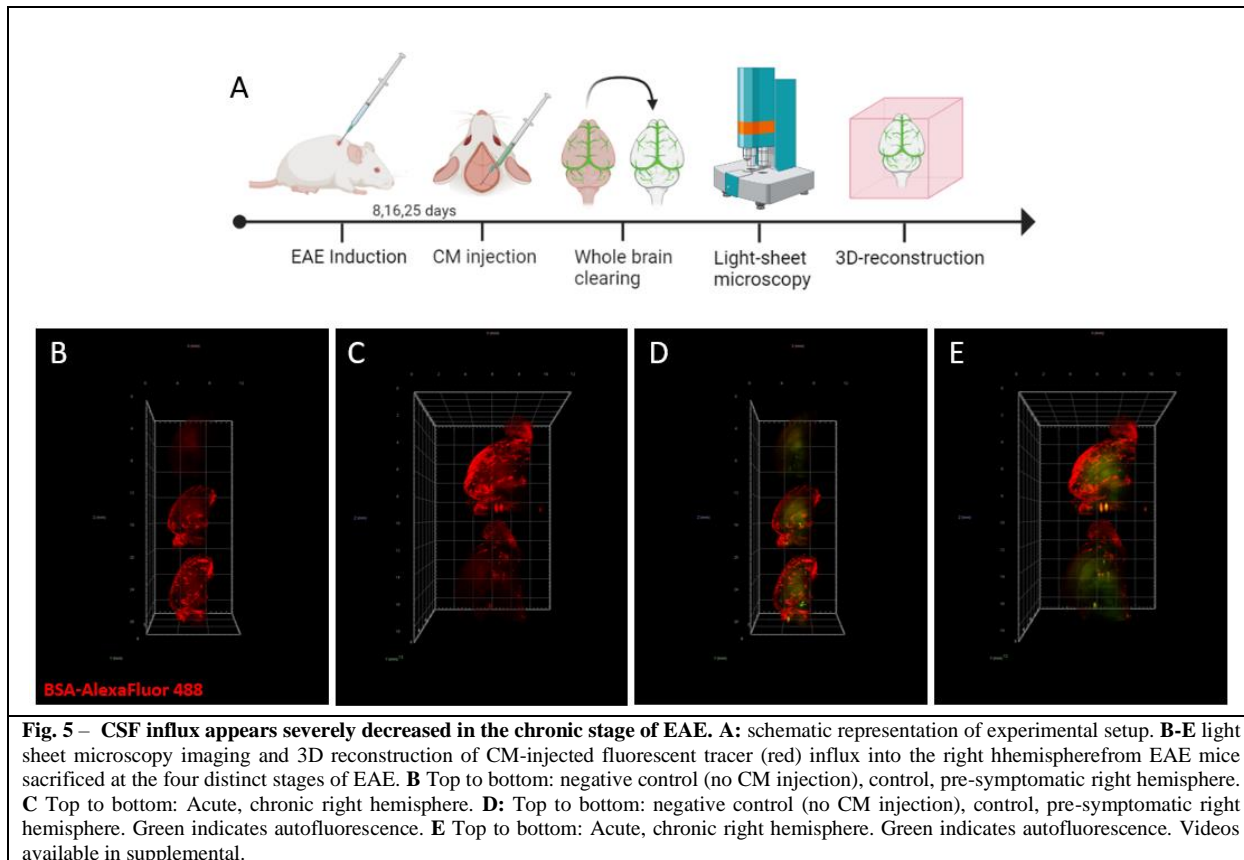


Fig. 5 – CSF influx appears severely decreased in the chronic stage of EAE. **A:** schematic representation of experimental setup. **B-E** light sheet microscopy imaging and 3D reconstruction of CM-injected fluorescent tracer (red) influx into the right hemisphere from EAE mice sacrificed at the four distinct stages of EAE. **B** Top to bottom: negative control (no CM injection), control, pre-symptomatic right hemisphere. **C** Top to bottom: Acute, chronic right hemisphere. **D:** Top to bottom: negative control (no CM injection), control, pre-symptomatic right hemisphere. Green indicates autofluorescence. **E** Top to bottom: Acute, chronic right hemisphere. Green indicates autofluorescence. Videos available in supplemental.

extravasation, suggesting that pericyte dysfunction may contribute to BBB disruption in EAE (Figure 3H).

Extending our investigations beyond the dorsal cortex, we conducted similar analyses on the thoracic spinal cord of mice sacrificed at different time points following EAE induction (Figure 4A). Interestingly, contrasting the findings in the dorsal cortex, we observed an increased total EB dye signal in the thoracic spinal cord specifically during the acute phase of EAE (Figure 4B). This suggests a distinct pattern of BBB permeability dynamics between these regions. Furthermore, we observed that the total EB signal returned to baseline levels in the chronic stage of the EAE model, indicating a reduction in BBB leakage at this stage (Figure 4B). Given the vascular changes observed in the thoracic spinal cord (Figure 1G) we performed an additional analysis that takes the total lectin+ area into account, to ensure accurate assessment of EB dye extravasation, considering the apparent binding of EB dye to the blood vessel wall. Following the correction for the total vessel signal, we found no evidence of ongoing leakage in the thoracic spinal

cord (Figure 4C). Therefore, the observed increase in the EB signal during the acute phase might be attributed to these vascular abnormalities rather than ongoing BBB leakage. On the contrary, this correlation between the increased lectin+ area and total EB dye, not seen in the dorsal cortex, might suggest that vascular abnormalities contribute to the increased EB signal in the thoracic spinal cord. Finally, we examined the relationship between the total EB dye signal and pericyte vessel coverage in the thoracic spinal cord. The observed negative correlation suggests that a higher pericyte vessel coverage is associated with a lower total EB dye signal, indicating reduced BBB permeability and a more effective restriction of EB extravasation (Figure 4D). This further strengthens the notion that pericytes are crucial for the maintenance of BBB integrity. In aggregate, these findings underscore the importance of considering region- specific and temporal factors in studying BBB permeability and highlight the critical role of pericytes as key regulators of this dynamic process.

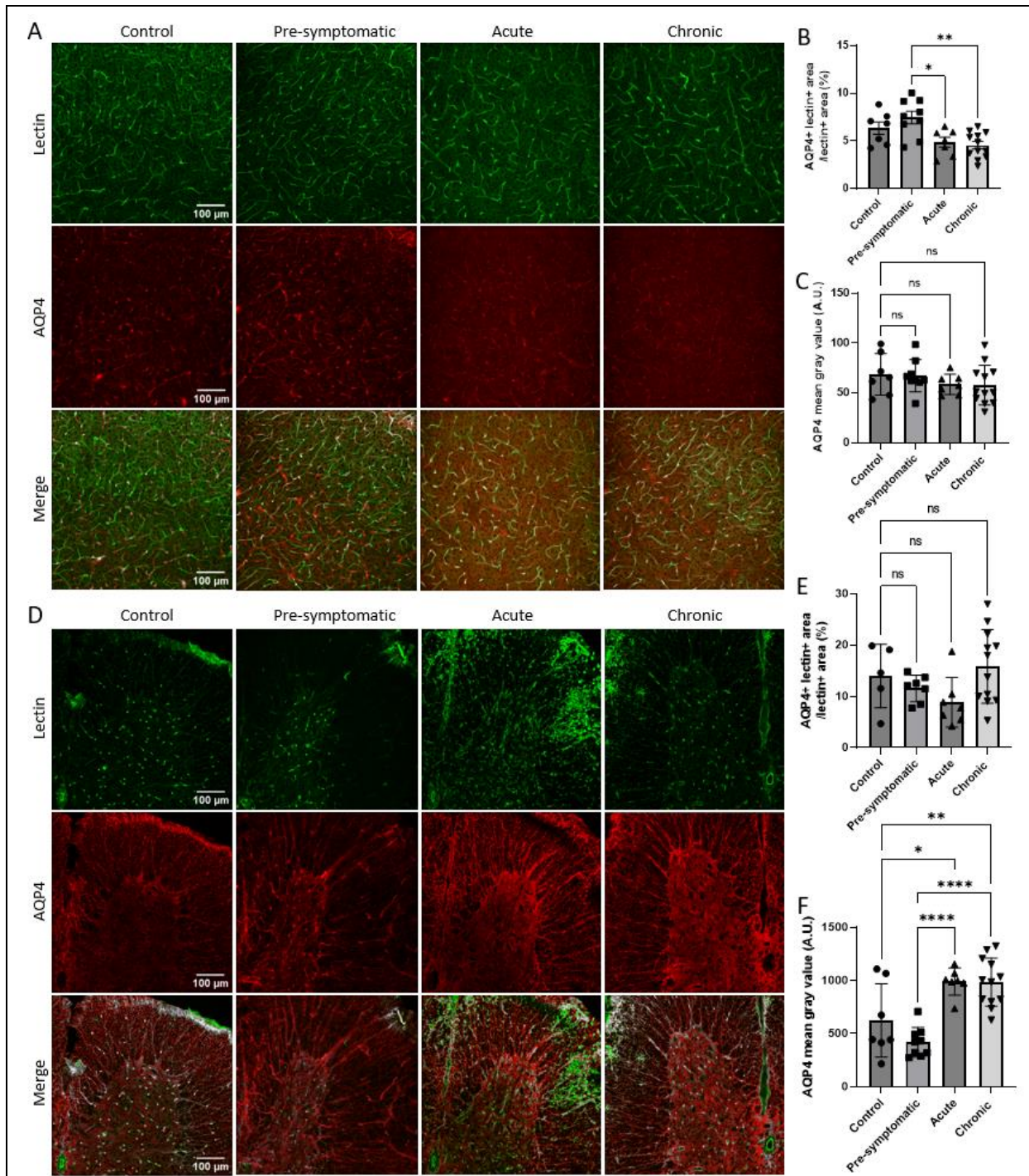
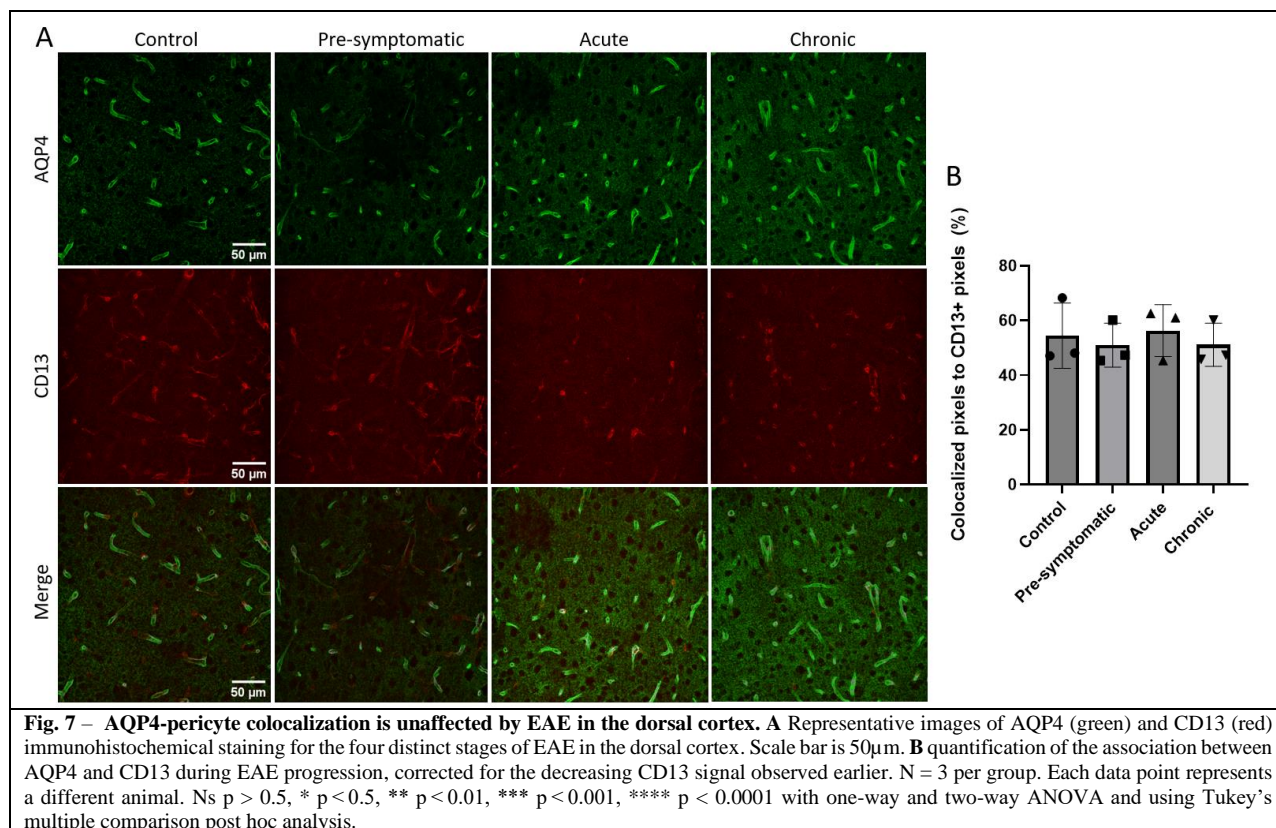


Fig. 6 – AQP4 vessel association is lost in the dorsal cortex, and its expression is upregulated in the thoracic spinal cord following EAE induction. **A** Representative images of lectin (green) staining for blood vessels and AQP4 (red) immunohistochemical staining for the four distinct stages of EAE in the dorsal cortex. Scale bar is 100µm. **B** Quantification of the AQP4 blood vessel association. **C** Quantification of AQP4+ area in the dorsal cortex. **D** Representative images of lectin (green) staining and AQP4 (red) immunohistochemical staining for blood vessels and pericytes respectively for the four distinct stages of EAE in the thoracic spinal cord. Scale bar is 100µm. **E** Quantification of the AQP4 blood vessel association. **F** Quantification of AQP4+ area in the dorsal cortex. **A-F** Average N = 9 per group. Each data point represents a different animal. *Ns* $p > 0.5$, * $p < 0.5$, ** $p < 0.01$, *** $p < 0.001$, **** $p < 0.0001$ with one-way and two-way ANOVA and using Tukey’s multiple comparison post hoc analysis.



CSF influx appears severely decreased in the chronic stage of EAE

As previously mentioned, dysfunction of the glymphatic system has been observed in MS patients, however this has not yet been thoroughly investigated in the EAE mouse model yet. Given our findings of decreased AQP4 vessel colocalization in the EAE model, this is worth exploring further. In this experiment EAE-induced mice at different stages of the disease were CM injected with Alexa-488 labeled BSA to investigate CSF influx. Here our results show that there appears to be large decrease in the CSF influx at the chronic stage of the disease compared to the control, pre-symptomatic and acute stage of the disease (Figure 5A-D, supplemental videos 1-2). These findings suggest glymphatic impairment specifically at the chronic stage, while this is not yet seen in the acute stage of the disease.

AQP4 vessel association is lost in the dorsal cortex, and its expression is upregulated in the thoracic spinal cord following EAE induction

The glymphatic system has emerged as a critical player in maintaining CNS homeostasis and waste

clearance (14). Although glymphatic system dysfunction has been observed in MS patients, and now the EAE model, its origin remains poorly understood (13). Emerging evidence suggests that aquaporin-4 (AQP4), a water channel protein highly expressed in astrocyte endfeet at the BBB interface, plays a significant role in glymphatic function (27). Its polarized distribution at astrocyte endfeet is crucial for maintaining water homeostasis and facilitating glymphatic clearance (27, 28). Disruption in AQP4 expression or localization has been associated with impaired glymphatic function and compromised waste clearance mechanisms (16). However, the impact of EAE induction on the expression pattern of AQP4 remains largely unexplored.

In this experiment, we aimed to investigate the vessel association and expression pattern of AQP4 in the dorsal cortex and thoracic spinal cord of EAE mice, sacrificed at different disease stages. To assess AQP4 vessel association, we performed immunohistochemical staining for AQP4 and labeled blood vessels with Dylight-488 labeled Tomato Lectin. In the dorsal cortex, we observed a decreased colocalization of AQP4 with blood

vessels in the acute and chronic phase compared to the pre-symptomatic group, suggesting a slight increase in the pre-symptomatic phase, followed by a loss of AQP4 (Figure 6B). Interestingly, this loss of vessel colocalization was not accompanied by a decrease in the overall mean fluorescence intensity of AQP4 (Figure 6C), suggesting that while the total expression levels remained unchanged, the proper distribution of AQP4 at the blood vessels was disrupted in the cortex of EAE mice. Moving to the thoracic spinal cord, we found no significant change in AQP4 vessel colocalization across different time points post induction (Figure 6E). However, we noted a significant increase in the total expression of AQP4 in the progressive stages of EAE compared to the control and pre-symptomatic phase (Figure 6F). This suggests that while AQP4 vessel colocalization may remain relatively stable in the spinal cord during EAE, there is an upregulation of AQP4 expression, possibly reflecting an adaptive response to the ongoing neuroinflammatory processes.

The association between AQP4 and pericytes remains unaffected by EAE induction in the dorsal cortex

Although recent studies have suggested a potential role of pericytes in the vessel colocalization of AQP4, this aspect has not yet been thoroughly explored in the context of EAE (29). Interestingly, our preliminary findings indicate the presence of pericyte dysfunction and loss of AQP4 vessel association in the EAE model, making it relevant to further explore the potential connection between pericytes and AQP4 expression patterns. In this experiment we aimed to investigate the potential impact of EAE induction on the regulatory role of pericytes in the expression of AQP4 at the neurovascular unit. To accomplish this, we performed an immunohistochemical staining for CD13, a marker for pericytes, as well as AQP4. (Figure 7A) Here, we assess the degree of colocalization between AQP4 and CD13, which serves as an indicator of whether pericytes retain their ability to influence local AQP4 expression. Important to note is that for this we considered the previously established reductions in both the overall CD13 expression and pericyte count. Our findings revealed no significant differences in the percentage of colocalized AQP4 and CD13 compared to the total CD13 expression (Figure 7B).

This suggests that the association between AQP4 and pericytes remains unaffected by the induction of EAE.

DISCUSSION

Pericytes play a crucial role in maintaining the integrity and functionality of the neurovascular unit, however their specific involvement in EAE pathogenesis has remained elusive (9, 30). Limited knowledge about pericyte alterations and their functional significance in the context of EAE limits our understanding of the complex interplay between neuroinflammation, vascular dysfunction, glymphatic dysfunction and disease progression. Therefore, it is evident that further investigation is needed to elucidate the role of pericytes in EAE and to uncover the underlying mechanisms that drive their alterations during disease progression. The initial findings of this paper show a significant decrease in the expression of the pericyte marker CD13 in the dorsal cortex as the EAE model progressed, already indicating potential alterations. Further examination revealed a reduction in both the pericyte count and pericyte blood vessel coverage, suggesting a disruption in their total population and association with blood vessels. Unfortunately it remains unknown what causes this pericyte disruption in the dorsal cortex. Several factors may be implicated in this. We speculate that the secretion of inflammatory mediators released during the immune response could impact pericyte adhesion and survival. Alternatively, alterations in the extracellular matrix (ECM) components of the neurovascular unit might contribute to the reduction in pericyte coverage (19, 31). The ECM provides structural support and facilitates crosstalk between the components of the BBB. Disruptions of ECM components during EAE could negatively affect pericyte adhesion and function. Future research on these potential factors could elucidate the underlying mechanisms driving pericyte disruption in EAE. In contrast to the cortex, we did not observe a decrease in CD13 expression or in the spinal cord. However, there was a significant decrease in pericyte blood vessel coverage. This observed decrease in pericyte blood vessel association, despite the absence of a decrease in the expression of the pericyte marker CD13, suggests the possibility of pericyte detachment from the blood vessels. Previous studies exploring hypoxic-stress and neuroinflammation related conditions have

demonstrated that pericytes are capable of migrating away from blood vessels (32, 33, 34). Our research group has uncovered significant hypoxia within the spinal cord in the context of the EAE model (12). Considering these findings, it is plausible that pericytes undergo detachment from blood vessels in response to the hypoxic microenvironment within the spinal cord during EAE. Moving on, during the acute phase of the EAE model, there was a large increase in the vascular density, suggesting vascular abnormalities. Similar vascular changes were seen during the chronic phase, although this was not significant following quantification. These findings diverge from our research group's previous results, which demonstrated reduced vascular length, radius, and bifurcations in the spinal cord following EAE induction (12). It is important to note that these findings were based on lectin perfusion rather than lectin staining, which only stains blood vessels that are still actively perfused while previous studies have shown that the spinal cord is hypo perfused during the acute and chronic phases of EAE (35). In addition to this, while lectins are commonly used to stain blood vessels, they can also stain microglia. This is known to be intensified during neuroinflammation, which is attributed to the upregulation of galactin-1 and other carbohydrate structures on the surface of activated microglia in MS lesions (36). However, this fails to explain the significant co-localization between CD31 staining and the lectin staining we conducted to validate the lectin's specificity during the acute stage of in the spinal cord. Furthermore, considering the critical role of pericytes in regulating angiogenesis and vascular stability, it is possible that altered expression or activity of angiogenic factors, such as vascular endothelial growth factor (VEGF) or platelet-derived growth factor (PDGF), might disturb angiogenesis. Therefore, it is important to consider that in the thoracic spinal cord, the observed decrease in pericyte vessel coverage might be attributed to vascular alterations rather than pericyte migration. To investigate how these pericyte changes affect the BBB, we focus on the involvement of pericytes in the regulation of claudin-5, a key tight junction protein for the maintenance of BBB integrity (11, 37). Our results show that claudin-5 expression is lost at the blood vessels during EAE disease progression. This was seen in conjunction with the

loss of pericyte blood vessel coverage. These data provide evidence that pericytes play a role in maintaining claudin-5 expression at the BBB interface, and that EAE induction negatively affects their function in this regard. Not much is known about how pericytes regulate claudin-5 expression. A recent study by Grygorowycz et al. (38) has shown that after EAE induction, pericytes increase their expression of P2XR7 (ATP-gated P2X receptor cation channel), which in turn correlated with decreased expression of claudin-5 (10, 38). They subsequently found that this loss of claudin-5 expression could be rescued with the administration of a P2XR7 agonist. A different study conducted by Shimizu et al. (39) revealed that glial cell line-derived neurotrophic factor (GDNF) and basic fibroblast growth factor (bFGF) are capable of enhancing the integrity of the BBB by promoting the expression of claudin-5 on endothelial cells. Interestingly, they found that pericytes are responsible for secreting these factors. Furthermore, they found that inhibition of the secretion of GDNF and bFGF by pericytes resulted in a decrease in claudin-5 expression. These studies suggest that P2XR7 activation in pericytes and GDNF and bFGF secretion by pericytes may play a role in modulating claudin-5 expression during EAE. However, further research is needed to fully understand the underlying mechanism between claudin-5 expression and pericytes in EAE and to validate these findings.

Our results already indicate impairment of the BBB due to pericyte lost and subsequent downregulation of the most crucial tight-junction protein, claudin-5. Next, we investigated the function impact of pericyte dysfunction on the BBB by examining the extravasation of EB dye, as a marker of BBB disruption. To this end, we administered IP injections of EB dye, after which we studied the fluorescence intensity of the EB dye in the brain and the spinal cord of EAE mice at different stages in the disease. It is worth noting that the EB extravasation method has been used in previous studies to measure BBB disruption in EAE. For instance, studies by Hamana and Wang et al. (40, 41) use EB dye to measure the effectivity of BBB enhancing treatments by comparing the EB dye intensity between control and treatment groups. However, our study aims to expand upon the existing literature by examining BBB leakage at different time points following EAE induction, to

identify the stage at which BBB integrity is significantly disrupted. Additionally, we will correlate these measurements of EB dye leakage with assessments of pericyte dysfunction to elucidate the role of pericytes in BBB integrity loss. To the best of our knowledge, no prior studies have employed this methodology to investigate the temporal dynamics of BBB leakage in EAE or explored its connection with pericyte dysfunction. Our findings indicate that in the dorsal cortex, most EB dye leakage can be found during the pre-symptomatic phase of EAE. This indicates that the loss of BBB integrity occurs early in the disease progression, even before the onset of any observable motor deficits. Furthermore, when we accounted for any vascular changes, we observed significant EB dye leakage during the acute phase in addition to the pre-symptomatic phase. However, as the disease progressed to the chronic phase, we noted a return to baseline levels of EB dye leakage. This suggests that the BBB recovers its integrity following the resolution of the acute phase of neuroinflammation. Interestingly, other studies have similarly found that the infiltration of immune cells into the CNS start from the pre-symptomatic phase (42). However, these studies also demonstrated an ongoing presence of immune cell infiltration in the CNS during the chronic phase of EAE, indicating that the relative amount of immune cells in the CNS continues to increase over time, despite our findings of apparent recovery of the BBB. Additionally, we discovered a significant negative correlation between the intensity of the EB dye in the cortex and the coverage of pericytes on the blood vessels. This correlation highlights the crucial role played by pericytes in maintaining BBB integrity. It suggests that the loss of pericyte association with blood vessels may lead to BBB leakage. We speculate that this might aggravate disease progression via immune cell infiltration, resulting in subsequent neuroinflammation, and edema. In regards to this, a very recent study has found that pericytes are also able to directly regulate infiltration of immune cells into the CNS. This was established by quantifying the total amount of immune cells in the brain parenchyma of pericyte-deficient EAE mice. This shows that pericytes are also capable of directly regulating endothelial transcytosis, emphasizing their significance in maintaining BBB integrity and regulating immune responses within the CNS (43).

Moving on to the thoracic spinal cord, we notice a significant increase in the EB dye extravasation only during the acute phase of EAE. Similarly as in the dorsal cortex, we notice that the EB dye in the spinal cord during the chronic phase returned to baseline. Given that EB dye seems to bind to the blood vessel wall, which has not been described in literature before, we corrected for changes in the vascular density. Here we noticed that after correction, no more significant changes in the EB dye signal remained. This indicates that in the thoracic spinal cord, the noticeable increase in EB dye extravasation might be attributed to an increase in the vessel density. This finding contrasts with our research groups current understanding, which suggests a decrease in vessel diameter and length following EAE induction (12). However, it is worth noting that different studies have reported conflicting results regarding vascular changes in the EAE model. A study conducted by Seabrook et al. (44) proposes that there is an increase in vessel density specifically during the chronic phase of EAE, while no observable changes occur during the acute phase. Conversely, Boroujerdi et al. (45) suggest that vascular remodelling already takes place in the spinal cord during the pre-symptomatic phase. They observed a significant increase in CD31+ blood vessels at this stage, which continued to rise as the disease model progressed. These contradictory findings show the complexity and variability of vascular changes within the spinal cord during EAE. It is evident that further research is needed to shed some light on these conflicting reports and gain a better understanding of the vascular changes occurring in the spinal cord at the various stages of EAE.

Finally, we aimed to explore the involvement of pericytes in the functioning of the glymphatic system within the EAE mouse model. Previous research by Carotenuto et al. (13) has indicated impaired glymphatic system function in MS patients. However, there has only been one investigation in EAE mouse model prior to our study, which is by Fournier et al (46). Our findings reveal a significant impairment of the glymphatic system in EAE, as indicated by a decrease influx of a fluorescent tracer, injected into the cisterna magna, during the chronic phase of the disease. These findings align with the decrease in pericyte coverage we notice in the chronic phase, however this was also present in the acute phase already. On

the contrary, there seems to be a slight increase in CSF influx in the acute phase, however we cannot confirm the significance of this as we lack sample size for this experiment. These findings are consistent with previous findings of Fournier et al, they found no significant decrease in CSF influx in the brain of EAE mice in the acute phase, however they unfortunately did not assess CSF influx at other stages of the disease, such as the chronic phase (46). Moving on, the underlying mechanisms contributing to this impairment have remained elusive. One crucial component of the glymphatic system is AQP4. It has been hypothesized that disturbances in cerebrospinal fluid circulation occur due to reduced AQP4 delocalization from the blood vessels (27)(14). To investigate this further, we first examined the total expression of total AQP4 in the dorsal cortex of the brain and found no significant changes during disease progression. However, we did observe a loss of AQP4 association with blood vessels, which correlated with a decrease in pericyte coverage. This observation aligns with existing literature suggesting that pericytes play a role in regulating AQP4 polarization on astrocyte endfeet. For instance, Gundersen et al. (29) revealed strong AQP4 signal in astrocytic processes adjacent to pericytes. However this has not been studied in the context of EAE. These results of diffuse AQP4 expression in EAE also corroborate the similar previous findings from Rohr et al. (47) However, it is not in line with previous findings from Fournier et al. who found no delocalization of AQP4 in the brain of EAE mice (46). To further investigate this connection between pericytes and AQP4, we performed colocalization analysis. Our results demonstrate that, considering the decreased pericyte count, pericytes display equal colocalization with AQP4 during the progression of EAE. This suggests that pericytes retain their ability to regulate AQP4 vessel association. Therefore, the decrease in their total number might be the driving force behind the reduction in AQP4 vessel association.

Similar analyses were conducted on the thoracic spinal cord,. Contrary to our findings in the dorsal cortex, we here found a large increase in AQP4 expression. In addition to this, there was no loss of AQP4 blood vessel association, likely due to their upregulation. Notably, this upregulation of AQP4 in the spinal cord in the EAE model has been

described before by Fournier et al (46). On the other hand, they found a decrease in AQP4 blood vessel association in the spinal cord of EAE mice (46). What leads to this upregulation of AQP4 in EAE remains unknown, however, studies of AQP4 in other neuroinflammatory disease provide some insight. Li et al. (48) has found AQP4 expression is highly linked to neuroinflammation, showcasing in their study that knockout of AQP4 led to reduced neuroinflammation in EAE mice that were passively induced. Furthermore, in spinal cord injury it is known that loss of AQP-4 has been associated with reduced spinal edema and improved prognosis (49). This increase in AQP4 falls in line with the highly increased EB dye extravasation that we observed in the thoracic spinal cord, both indicating acute neuroinflammation. Unfortunately, the mechanism whereby AQP4 becomes upregulated in the spinal cord, and how this contributes to neuroinflammation apart from likely enhancing edema and cytokine release has remained elusive and indicates a clear need for more research on this topic.

CONCLUSION

Our study reveals significant alterations in three key aspects related to neurovascular function in EAE. Firstly, we observed a notable decrease in pericyte blood vessel coverage, suggesting EAE negatively impacts pericyte viability, which could result in neurovascular instability. This was paired with a marked increase of BBB leakage, indicating the role of pericyte dysfunction in compromised barrier integrity and enhanced permeability in EAE. Lastly, a decrease in glymphatic function was observed, suggesting impaired clearance of waste metabolites and potential disruption of interstitial fluid dynamics in the brain. The findings provide valuable insights into the pathophysiological mechanisms underlying this MS. Further investigations are warranted to further explore the causal relationships and potential therapeutic interventions targeting these pericyte-related alterations.

Acknowledgements

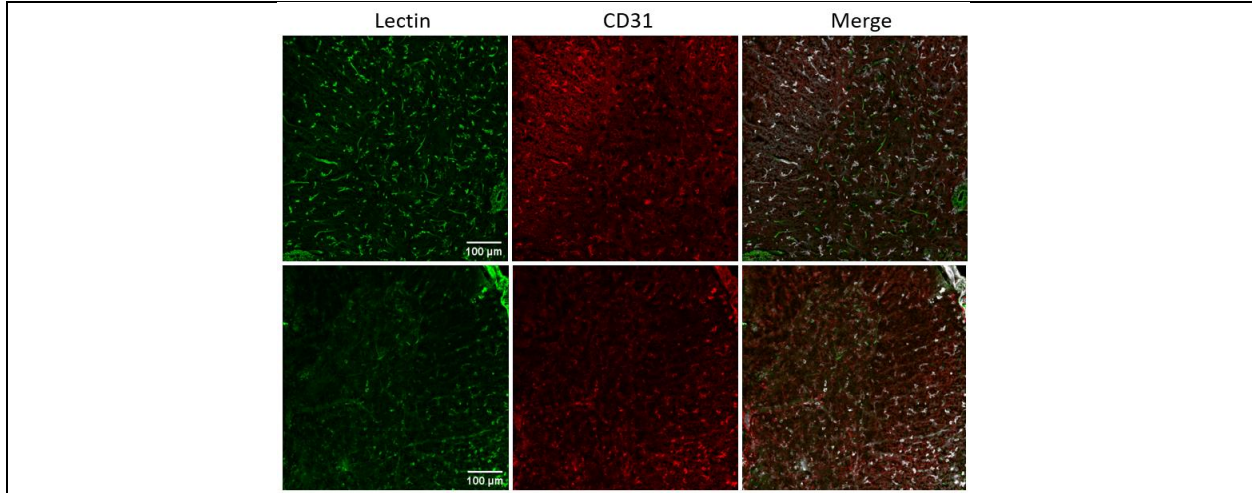
I would like to thank both my daily supervisor Na Liu and my promotor Iben Lundgaard for their excellent guidance and throughout this internship. I am truly grateful for the opportunity to have worked under their mentorship. I would also like to thank

the other members of the Glia-Immune Interactions lab for the engaging discussions and their insightful perspectives on the project. Lastly I am grateful to all those who have contributed in any way to make this Erasmus internship a valuable and enriching experience.

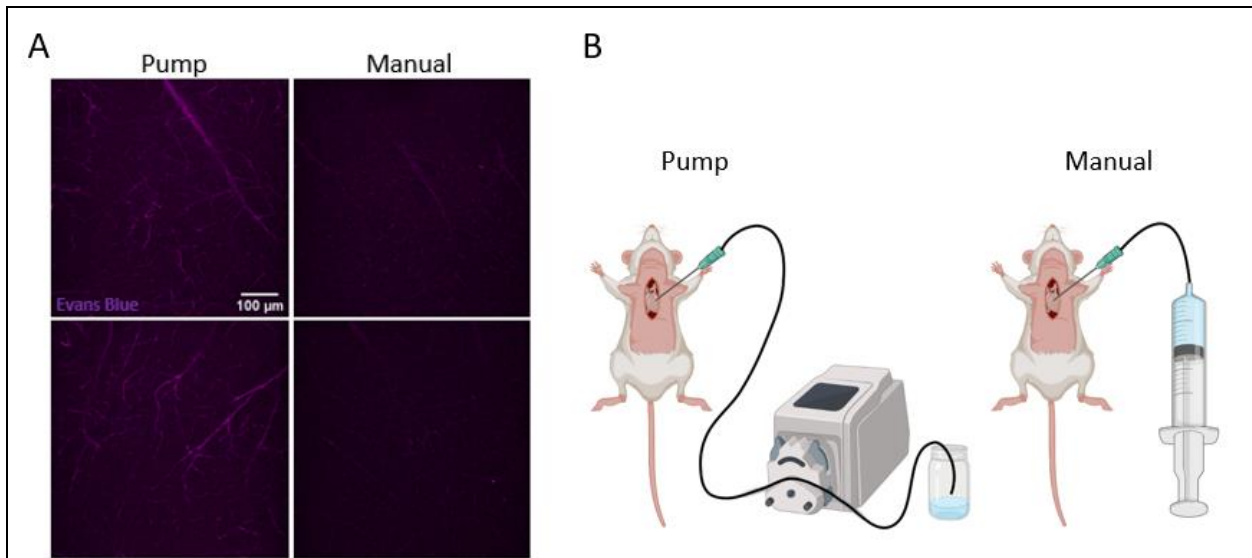
Author contributions

BM, NL, IB conceived the experiments. BM, NL performed the experiments. BM, NL, IL, discussed results. BM wrote the manuscript. NL and IL revised the manuscript.

SUPPLEMENTAL FIGURES



Supplemental fig. 1 – Lectin colocalizes with CD31 in the spinal cord of the acute phase of EAE, indicating vessel specificity at this stage. Representative images of lectin (green) staining for blood vessel and CD31 (red) immunohistochemical staining for vascular endothelial cells in the thoracic spinal cord from EAE mice sacrificed at the acute stage. Scale bar is 100µm.



Supplemental fig. 2 – Manual transcordial perfusion more effectively removes remaining EB dye and does not induce artificial BBB leakage. **A** representative confocal microscopy images of the dorsal cortex of mice injected with EB, comparing the fast manual method to the slow peristaltic pump transcordial perfusion. **B** Visual representation of the manual method and the peristaltic pump transcordial perfusion method.

Primary antibodies	Secondary antibodies
Rat anti-CD13 (1:300, MCA2183, Bio-Rad)	Donkey anti-rat 568 (1:500, ab175475 Abcam)
Rabbit anti-PDGFRb (1:300, 14-1402-82, eBioscience)	Donkey anti-rabbit 568 (1:500, 10617183, Invitrogen)
Rabbit anti-Claudin-5 (1:300, XD34254, Fisher Scientific GFT AB)	Donkey anti rabbit 488 (1:500, A21206, Invitrogen)
Rabbit anti CD31 (1:300, ab28364, Abcam)	
Rabbit anti AQP4 (1:300, AB3594, Merck)	
Supplemental table 1: Primary and respective secondary antibodies used during this study (concentration, catalogue number, company).	

SUPPLEMENTAL VIDEOS:

Supplemental video 1:

<https://drive.google.com/file/d/1gcTpBYO8PYdJYGC7rcdtNPqxiBSqcEg6/view?usp=sharing>

Supplemental video 2:

<https://drive.google.com/file/d/1IC-JdfXEtqeUD4rL003XVUgZ9eDluK7B/view?usp=sharing>

REFERENCES

- Ghasemi N, Razavi S, Nikzad E. Multiple Sclerosis: Pathogenesis, Symptoms, Diagnoses and Cell-Based Therapy. *Cell J.* 2017;19(1):1-10.
- Dobson R, Giovannoni G. Multiple sclerosis - a review. *Eur J Neurol.* 2019;26(1):27-40.
- Miller DH, Leary SM. Primary-progressive multiple sclerosis. *Lancet Neurol.* 2007;6(10):903-12.
- Ontaneda D, Fox RJ. Progressive multiple sclerosis. *Curr Opin Neurol.* 2015;28(3):237-43.
- Havrdova E, Horakova D, Kovarova I. Alemtuzumab in the treatment of multiple sclerosis: key clinical trial results and considerations for use. *Ther Adv Neurol Disord.* 2015;8(1):31-45.
- GAY D, ESIRI M. BLOOD-BRAIN BARRIER DAMAGE IN ACUTE MULTIPLE SCLEROSIS PLAQUES: AN IMMUNOCYTOLOGICAL STUDY. *Brain.* 1991;114(1):557-72.
- Ortiz GG, Pacheco-Moisés FP, Macías-Islas M, Flores-Alvarado LJ, Mireles-Ramírez MA, González-Renovato ED, et al. Role of the blood-brain barrier in multiple sclerosis. *Arch Med Res.* 2014;45(8):687-97.
- Daneman R, Prat A. The blood-brain barrier. *Cold Spring Harb Perspect Biol.* 2015;7(1):a020412.
- Brown LS, Foster CG, Courtney J-M, King NE, Howells DW, Sutherland BA. Pericytes and Neurovascular Function in the Healthy and Diseased Brain. *Frontiers in Cellular Neuroscience.* 2019:NA.
- Rivera FJ, Hinrichsen B, Silva ME. Pericytes in Multiple Sclerosis. *Adv Exp Med Biol.* 2019;1147:167-87.
- Armulik A, Genové G, Mäe M, Nisancioglu MH, Wallgard E, Niaudet C, et al. Pericytes regulate the blood-brain barrier. *Nature.* 2010;468(7323):557-61.
- Ramos-Vega M, Kjellman P, Todorov MI, Kylkilahti TM, Bäckström BT, Ertürk A, et al. Mapping of neuroinflammation-induced hypoxia in the spinal cord using optoacoustic imaging. *Acta Neuropathol Commun.* 2022;10(1):51.
- Carotenuto A, Cacciaguerra L, Pagani E, Preziosa P, Filippi M, Rocca MA. Glymphatic system impairment in multiple sclerosis: relation with brain damage and disability. *Brain.* 2022;145(8):2785-95.
- Jessen NA, Munk AS, Lundgaard I, Nedergaard M. The Glymphatic System: A Beginner's Guide. *Neurochem Res.* 2015;40(12):2583-99.
- Illiff JJ, Wang M, Liao Y, Plogg BA, Peng W, Gundersen GA, et al. A Paravascular Pathway Facilitates CSF Flow Through the Brain Parenchyma and the Clearance of Interstitial Solutes, Including Amyloid β . *Science Translational Medicine.* 2012;4(147):147ra11-11.
- Benveniste H, Liu X, Koundal S, Sanggaard S, Lee H, Wardlaw J. The Glymphatic System and Waste Clearance with Brain Aging: A Review. *Gerontology.* 2019;65(2):106-19.
- Lampron A, Laroche A, Laflamme N, Préfontaine P, Plante MM, Sánchez MG, et al. Inefficient clearance of myelin debris by microglia impairs remyelinating processes. *J Exp Med.* 2015;212(4):481-95.
- Neumann H, Kotter MR, Franklin RJM. Debris clearance by microglia: an essential link

- between degeneration and regeneration. *Brain*. 2008;132(2):288-95.
19. Iliff JJ, Wang M, Zeppenfeld DM, Venkataraman A, Plog BA, Liao Y, et al. Cerebral arterial pulsation drives paravascular CSF-interstitial fluid exchange in the murine brain. *J Neurosci*. 2013;33(46):18190-9.
 20. Bilston LE, Stoodley MA, Fletcher DF. The influence of the relative timing of arterial and subarachnoid space pulse waves on spinal perivascular cerebrospinal fluid flow as a possible factor in syrinx development. *J Neurosurg*. 2010;112(4):808-13.
 21. Zambach SA, Cai C, Helms HCC, Hald BO, Dong Y, Fordsmann JC, et al. Precapillary sphincters and pericytes at first-order capillaries as key regulators for brain capillary perfusion. *Proceedings of the National Academy of Sciences*. 2021;118(26):e2023749118.
 22. Bèchet NB, Kylkilahti TM, Mattsson B, Petrasova M, Shanbhag NC, Lundgaard I. Light sheet fluorescence microscopy of optically cleared brains for studying the glymphatic system. *J Cereb Blood Flow Metab*. 2020;40(10):1975-86.
 23. Renier N, Adams EL, Kirst C, Wu Z, Azevedo R, Kohl J, et al. Mapping of Brain Activity by Automated Volume Analysis of Immediate Early Genes. *Cell*. 2016;165(7):1789-802.
 24. Zhang ZS, Zhou HN, He SS, Xue MY, Li T, Liu LM. Research advances in pericyte function and their roles in diseases. *Chin J Traumatol*. 2020;23(2):89-95.
 25. Hirunpattarasilp C, Attwell D, Freitas F. The role of pericytes in brain disorders: from the periphery to the brain. *J Neurochem*. 2019;150(6):648-65.
 26. Sun Z, Gao C, Gao D, Sun R, Li W, Wang F, et al. Reduction in pericyte coverage leads to blood-brain barrier dysfunction via endothelial transcytosis following chronic cerebral hypoperfusion. *Fluids and Barriers of the CNS*. 2021;18(1):21.
 27. Gomolka RS, Hablitz LM, Mestre H, Giannetto M, Du T, Hauglund NL, et al. Loss of aquaporin-4 results in glymphatic system dysfunction via brain-wide interstitial fluid stagnation. *eLife*. 2023;12:e82232.
 28. Munk AS, Wang W, Bèchet NB, Eltanahy AM, Cheng AX, Sigurdsson B, et al. PDGF-B Is Required for Development of the Glymphatic System. *Cell Rep*. 2019;26(11):2955-69.e3.
 29. Gundersen GA, Vindedal GF, Skare O, Nagelhus EA. Evidence that pericytes regulate aquaporin-4 polarization in mouse cortical astrocytes. *Brain Struct Funct*. 2014;219(6):2181-6.
 30. Sweeney MD, Ayyadurai S, Zlokovic BV. Pericytes of the neurovascular unit: key functions and signaling pathways. *Nat Neurosci*. 2016;19(6):771-83.
 31. Baeten KM, Akassoglou K. Extracellular matrix and matrix receptors in blood-brain barrier formation and stroke. *Dev Neurobiol*. 2011;71(11):1018-39.
 32. Nishioku T, Dohgu S, Takata F, Eto T, Ishikawa N, Kodama KB, et al. Detachment of brain pericytes from the basal lamina is involved in disruption of the blood-brain barrier caused by lipopolysaccharide-induced sepsis in mice. *Cell Mol Neurobiol*. 2009;29(3):309-16.
 33. Dore-Duffy P, Owen C, Balabanov R, Murphy S, Beaumont T, Rafols JA. Pericyte migration from the vascular wall in response to traumatic brain injury. *Microvasc Res*. 2000;60(1):55-69.
 34. Melgar MA, Rafols J, Gloss D, Diaz FG. Postischemic reperfusion: ultrastructural blood-brain barrier and hemodynamic correlative changes in an awake model of transient forebrain ischemia. *Neurosurgery*. 2005;56(3):571-81.
 35. Desai RA, Davies AL, Del Rossi N, Tachrount M, Dyson A, Gustavson B, et al. Nimodipine Reduces Dysfunction and Demyelination in Models of Multiple Sclerosis. *Ann Neurol*. 2020;88(1):123-36.
 36. Siew JJ, Chern Y. Microglial Lectins in Health and Neurological Diseases. *Front Mol Neurosci*. 2018;11:158.
 37. Greene C, Hanley N, Campbell M. Claudin-5: gatekeeper of neurological function. *Fluids and Barriers of the CNS*. 2019;16(1):3.
 38. Grygorowicz T, Dąbrowska-Bouta B, Strużyńska L. Administration of an antagonist of P2X7 receptor to EAE rats prevents a decrease of expression of claudin-5 in cerebral capillaries. *Purinergic Signal*. 2018;14(4):385-93.
 39. Shimizu F, Sano Y, Saito K, Abe M-a, Maeda T, Haruki H, et al. Pericyte-derived Glial Cell Line-derived Neurotrophic Factor Increase the Expression of Claudin-5 in the Blood-brain Barrier and the Blood-nerve Barrier. *Neurochemical Research*. 2012;37(2):401-9.

40. Hamana A, Takahashi Y, Tanioka A, Nishikawa M, Takakura Y. Amelioration of Experimental Autoimmune Encephalomyelitis in Mice by Interferon-Beta Gene Therapy, Using a Long-Term Expression Plasmid Vector. *Mol Pharm.* 2017;14(4):1212-7.
41. Wang D, Li SP, Fu JS, Zhang S, Bai L, Guo L. Resveratrol defends blood-brain barrier integrity in experimental autoimmune encephalomyelitis mice. *J Neurophysiol.* 2016;116(5):2173-9.
42. Nam J, Koppinen TK, Voutilainen MH. MANF Is Neuroprotective in Early Stages of EAE, and Elevated in Spinal White Matter by Treatment With Dexamethasone. *Front Cell Neurosci.* 2021;15:640084.
43. Török O, Schreiner B, Schaffenrath J, Tsai HC, Maheshwari U, Stifter SA, et al. Pericytes regulate vascular immune homeostasis in the CNS. *Proc Natl Acad Sci U S A.* 2021;118(10).
44. Seabrook TJ, Littlewood-Evans A, Brinkmann V, Pöllinger B, Schnell C, Hiestand PC. Angiogenesis is present in experimental autoimmune encephalomyelitis and pro-angiogenic factors are increased in multiple sclerosis lesions. *Journal of Neuroinflammation.* 2010;7(1):95.
45. Boroujerdi A, Welser-Alves JV, Milner R. Extensive vascular remodeling in the spinal cord of pre-symptomatic experimental autoimmune encephalomyelitis mice; increased vessel expression of fibronectin and the $\alpha 5\beta 1$ integrin. *Exp Neurol.* 2013;250:43-51.
46. Fournier AP, Gauberti M, Quenault A, Vivien D, Macrez R, Docagne F. Reduced spinal cord parenchymal cerebrospinal fluid circulation in experimental autoimmune encephalomyelitis. *J Cereb Blood Flow Metab.* 2019;39(7):1258-65.
47. Rohr SO, Greiner T, Joost S, Amor S, Valk PV, Schmitz C, et al. Aquaporin-4 Expression during Toxic and Autoimmune Demyelination. *Cells.* 2020;9(10).
48. Li L, Zhang H, Varrin-Doyer M, Zamvil SS, Verkman AS. Proinflammatory role of aquaporin-4 in autoimmune neuroinflammation. *Faseb j.* 2011;25(5):1556-66.
49. Pan Q-L, Lin F-X, Liu N, Chen R-C. The role of aquaporin 4 (AQP4) in spinal cord injury. *Biomedicine & Pharmacotherapy.* 2022;145:112384.